Does a head-forward posture produce neck dislocation during inverted drop experiments?

Ryan D. Quarrington, Mario Mongiardini, Aaron W. Stevenson, Ashish Diwan

Abstract Despite the established link between head-first impacts (HFI) and subaxial cervical facet dislocation (CFD), replicating this experimentally has proven challenging. The lack of a repeatable, dynamic exvivo model of CFD means there is limited mechanistic understanding of this injury, which is preventing improvements towards injury prevention, detection, and treatment. A recent computational study indicated that a head-forward posture (HFP) may elevate the risk of CFD during HFI, but this has not been confirmed experimentally. This study aims to develop an inverted HFI experimental model to explore whether a pre-impact HFP produces CFD, and to measure the associated head-neck kinematics and kinetics.

Keywords Cervical facet dislocation, drop tower, head-first impact, injury biomechanics, neck trauma.

I. INTRODUCTION

Subaxial cervical facet dislocation (CFD) is a severe neck injury that often results from torso compression following head-first impacts (HFI), such as during a motor vehicle rollover [1]. Despite the established causal link between HFI and CFD, and decades of laboratory research, replicating CFD in experimental HFIs has proven challenging. The lack of repeatable dynamic models of subaxial CFD highlights gaps in understanding of its underlying mechanisms, thereby hindering the advancement of effective injury prevention devices and strategies.

Prior laboratory investigations have produced subaxial CFD by applying quasi-static axial compression to C0-T1 specimens [2-3]. By permitting anterior C0 translation and maintaining a horizontal Frankfort Plane (FP) during these experiments, an 'S-shaped' or 'buckled' neck posture was produced, leading to CFD in the lower cervical spine. However, these head-end boundary conditions likely diverge from the dynamics of a real-life HFI event, where inertia resists head motion during the onset of neck injury [4]. Nonetheless, the eccentric head-forward posture (HFP) created in these quasi-static experiments might elevate the risk of CFD during an actual HFI.

The effect of varying anterior head eccentricity on subaxial cervical spine kinematics and kinetics during HFI was recently explored using dynamic finite element (FE) computer simulations [5]. Despite limitations in some tissue failure criteria of the head-neck model, the simulation results indicated that a pre-impact head eccentricity of greater than 20 mm, when the FP is horizontal, induced lower neck kinematics and kinetics likely to produce CFD. Therefore, the aims of this study were to: (A) develop a repeatable inverted drop HFI experiment capable of precisely varying pre-impact head eccentricity and FP angle; (B) validate whether pre-impact HFP reliably produces CFD; and (C) quantify the associated head-neck kinematics and kinetics during these experimental HFIs.

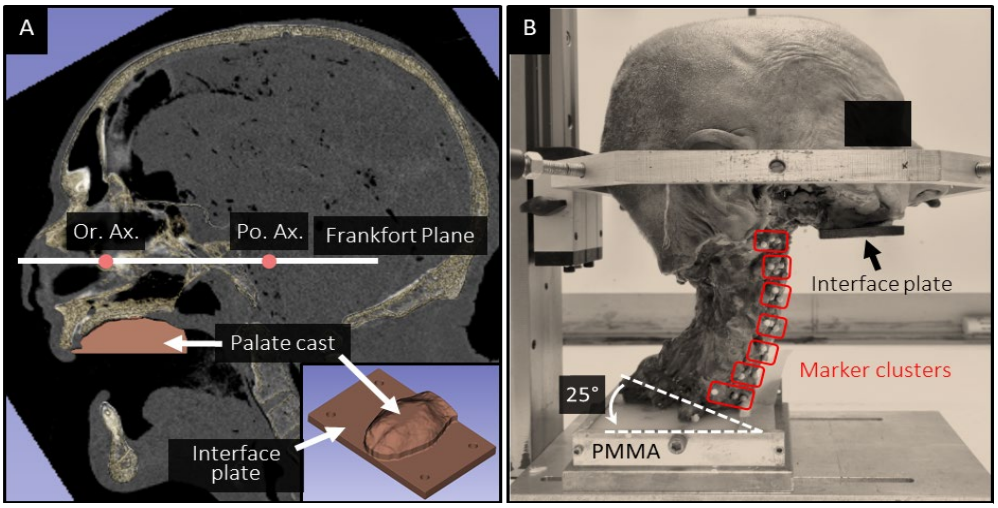

Fig. 1. (A) Specimen-specific, 3D-printed hard-palate interface plates aligned the Frankfort Plane landmarks (orbitale axis [Or. Ax.], porion axis [Po. Ax.]) with the horizontal. (B) T1 was embedded in a mould of polymethylmethacrylate (PMMA) at 25° to horizontal. Marker clusters were fixed to the cephalus and C1-T1 vertebrae.

R. D. Quarrington (tel: +61418560917; e-mail: ryan.quarrington@adelaide.edu.au) is a Research Fellow at Adelaide Medical School & Centre for Automotive and Safety Research (CASR), The University of Adelaide, Australia. M. Mongiardini is a Senior Research Fellow at CASR. A. Stevenson is Head of the Spinal Surgery Unit at Royal Adelaide Hospital (RAH). A. Diwan is Chair of Spinal Surgery at RAH and at The University of Adelaide.

II. METHODS

Specimen preparation

Institutional Human Research Ethics Committee approval was obtained (Reference No. H-2023-098). Four fresh-frozen post-mortem human subject (PMHS) (70M, 84F, 98M, 95M) head-neck specimens (cephalus-T1) were selected following review of screening computed tomography (CT) images for excessive degeneration, injury, disease, or prior surgery by a spine surgeon (AWS). Specimens were stored at -20°C and thawed at 4°C prior to preparation. Neck flesh, muscles, hyoid bone, and the mandible were removed to enable direct visualisation of C1 to T1. Hydration was maintained with phosphate buffered saline during storage and preparation. Specimen-specific hard palate casts were generated from the screening CT data using 3D Slicer (v5.0.3) and were 3D-printed onto an interface plate that aligned the Frankfort Plane to the required angle (nominally horizontal; Fig. 1A). The cast-plate unit was then rigidly fixed to the PMHS's hard palate with screws. T1 was augmented with screws and wire, and embedded in an aluminium mould using polymethylmethacrylate (PMMA; Kulzer, Hanau, Germany); the T1 neural canal was positioned centrally within the mould with the inferior endplate inclined at 25° to horizontal, approximating the supine in vivo sagittal angle [4]. Four reflective pin markers (4 mm diameter) were fixed to exposed bony surfaces of the cephalus and C1 to T1 (Fig. 1B). Pre-test CT images (NAEOTOM Alpha, Siemens, Munich, Germany; 0.2 mm isotropic voxels) were obtained of the PMMA-embedded and marker-instrumented specimen.

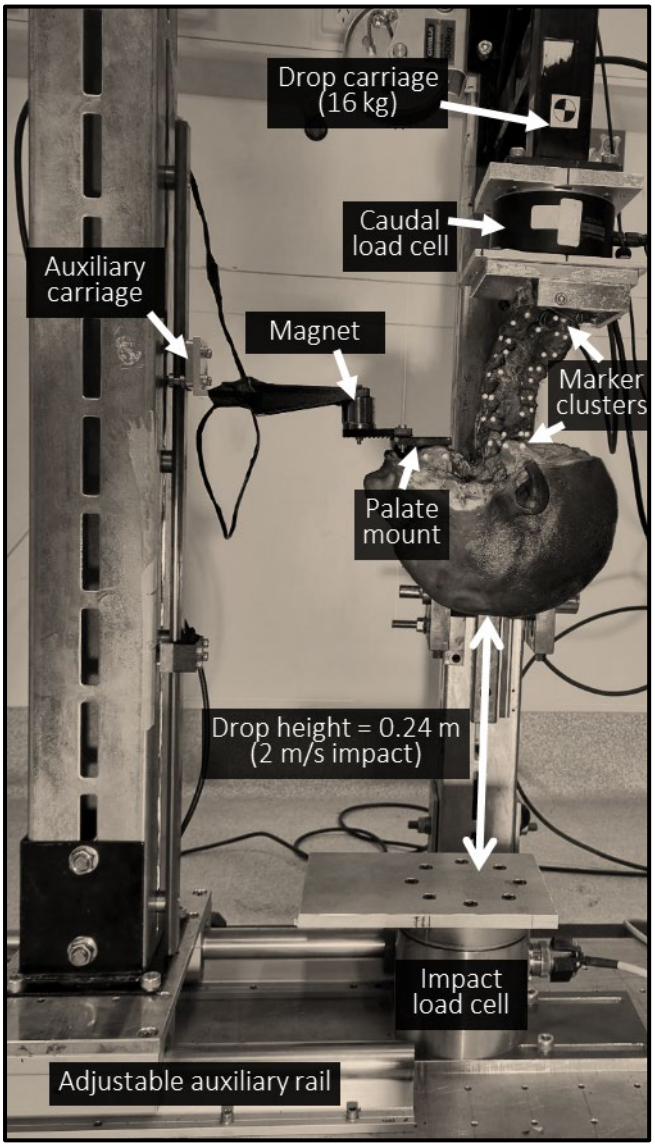

Fig. 2. Annotated photo of the inverted head-first impact drop test experimental setup.

Inverted drop and head-neck posture setup

Specimens underwent inverted HFI experiments using a custom drop-tower (Fig. 2). The T1 potting cup of the inverted specimen was attached to a six-axis load cell (K6D110 ±20 kN, ME, Hennigsdorf, Germany) on the underside of a torso-simulating carriage (16 kg mass [4]). A second six-axis load cell (MC5-2500, AMTI, MA, USA) measured impact surface loads. Drop-height (0.24 m for a 2 m/s head-impact velocity) was set by monitoring real-time output of a linear encoder (LM15, Rotary and Linear Motion Sensors, Slovenia) that measured drop carriage position. To set and maintain head eccentricity during the drop, the hard palate mount interfaced with an adjustable, auxiliary parallel drop rail and carriage via an electromagnet. The position of the auxiliary rail was adjusted using a lockable linear bearing to achieve the desired horizontal distance (nominally 30 mm) between the foramen magnum (FM) centre inferior-posterior corner of the T1 vertebral body (approximately centre of T1 potting mould). Head constraints were removed immediately prior to impact via external trigger release of the electromagnet.

Data acquisition and data processing

Load cell and carriage position data were collected synchronously at 50 kHz using a data acquisition system (PXIe-1073, BNC-2120, & PXIe-4331, National Instruments, USA) and custom LabVIEW code (2019, National Instruments, USA). Marker positions were captured with stereo-calibrated high-speed cameras (Phantom VEO1010; 10 kHz), which were synchronised with the other data streams via trigger signal. Data were processed

using custom MATLAB code (R2021b, Mathworks, MA, USA). Second-order, two-way, low-pass Butterworth filters were applied to the data per SAE J211 [6].

The relative locations of the pin markers and the anatomical landmarks and features (e.g. foramen magnum, Frankfort Plane) were identified from the pre-test CT using image analysis software (3D Slicer v5.0.3), and anatomical coordinate systems (ACS) were defined for the cephalus and each spinal level. Marker positional data were tracked and extracted (PCC 3.7, Vision Research Inc., Canada), then the dynamic motions for each marker set were applied to their respective ACS, assuming rigid-body motion. Three-dimensional global and segmental kinematics were calculated by deriving Euler angles and linear translations from affine transformations between ACS pairs at each frame [7]. Injuries were identified via post-test dissection and CT scan. The timepoint of each injury was identified from the synchronised high-speed camera footage and load cell data. Head-neck posture immediately prior to impact, and kinematics and kinetics at and preceding the injury timepoints, were extracted. Descriptive statistics were calculated.

III. RESULTS

Three of the four inverted HFI experiments had complete kinematic data; the C0 markers for specimen 5065 were obscured during impact, therefore skull kinematic parameters were not derived. For the three tests with skull position data, pre-impact eccentricity ranged from 28.4 mm to 35.7 mm and FP angle was 3.6° ± 3.8° to horizontal (Table I). Three of the four experiments resulted in bilateral C7/T1 CFD. The fourth specimen (5063) immediately fractured through the T1 vertebral body at head impact. Failure occurred at the embedded screw/vertebra interface in a region of low trabecular bone density, causing the specimen to fall away from the drop-tower without further injury. Kinematic and kinetic data were therefore omitted from analysis for this specimen.

TABLE I
SUMMARY OF SPECIMEN DONOR DEMOGRAPHICS AND KEY EXPERIMENTAL PARAMETERS

Specimen ID	Sex	Age (years)	Initial eccentricity (mm)	Initial FP angle (deg.)	Impact velocity (m/s)	CFD?	Fractures?
5052	M	70	28.4	-1.3	1.86	C7/T1	No
5065	F	84	-	-	2.04	C7/T1	Atlas & C4 SP
5064	M	98	30.5	7.8	2.04	C7/T1	C4 VB & T1 EP
5063	M	~~95~~	~~35.7~~	~~4.4~~	~~1.86~~	No	T1 VB
Average ± SD		84 ± 11	29.5 ± 1.1	*3.3 ± 4.6*	1.98 ± 0.08		

Note: FP = Frankfort Plane; CFD = cervical spine facet dislocation; SP = spinous process; VB = vertebral body; EP = endplate; Fx = fracture; SD = standard deviation. Strikethrough values were excluded from averages.

The kinematics, kinetics, and injury sequence leading to CFD was common for all three specimens (Table II and Fig. 3). Peak axial head impact force (5,619 ± 218 N) occurred ~2 ms post-impact, followed by peak axial torso force (1.32–1.67 kN) at 7.5–10 ms, which corresponded with failure of the C7/T1 interspinous ligament (ISL). Except for a small amount of vertical rebound, the head remained stationary during this period (Fig. 3A and B) and the neck adopted the S-shaped posture; upper neck (C0-C7) extension of 13.7° to 49.5° caused supraphysiologic C7/T1 flexion (18.3 ± 8.1°) and ISL rupture. No evidence of upper neck injury was observed on the video footage during this phase of the impact. Subsequent torso compression, plus head extension rotation and forward motion, caused additional C7/T1 flexion rotation and anterior shear translation (Fig. 3C), resulting in rupture of all intervertebral soft-tissues and CFD (Fig. 3D and E). Post-test dissection and CT revealed that CFD of specimens 5064 and 5065 occurred via fracture through the T1 superior endplate, and that no concomitant facet fractures were produced (Table II). Upper neck fractures were observed in two specimens, but analysis of the video footage identified that these were an artefact of C0-C5 hyperextension caused by drop-tower compression following the HFI phase of the experiments. No skull fractures occurred.

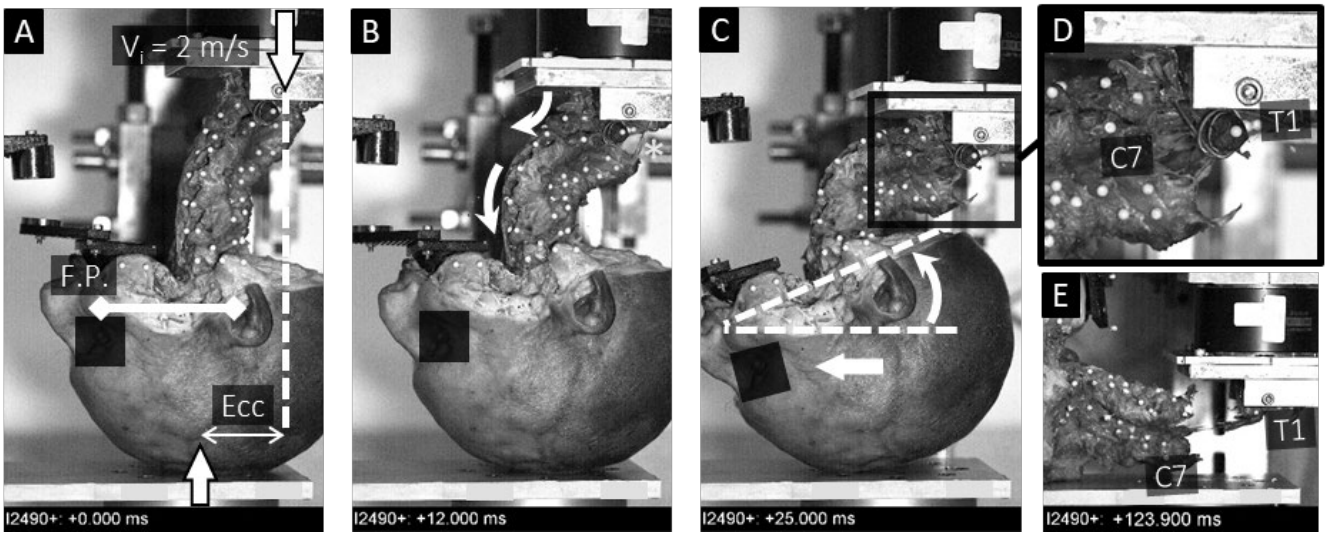

Fig. 3. Annotated high-speed video stills illustrating the CFD injury sequence (ID #5064). (A) At the point of impact (t = 0 ms), the head was arrested with a horizontal Frankfort Plane (FP) and an eccentric (Ecc) posture. (B) After 12 ms, carriage compression with minimal head motion produced an S-shaped neck and failure of the C7/T1 interspinous ligament (*). (C) At 25 ms post-impact, further torso compression, plus head extension and anterior translation, caused complete rupture of all C7/T1 soft-tissues (magnified in D), and CFD (E).

TABLE II
KEY EXPERIMENTAL OUTCOMES

Specimen ID	Peak axial impact force (kN)	T1 axial load at C7/T1 ISL failure (kN)	C0-C7 angle at ISL failure (deg.)	C7/T1 angle at ISL failure (deg.)	Peak C7/T1 shear force (N)
5052	5.32	1.67	-49.5	10.2	738
5065	5.83	1.38	-	14.4	617
5064	5.72	1.32	-13.7	26.4	746
Av ± SD	5.62 ± 0.22	1.46 ± 0.15	-31.6 ± 17.9	18.3 ± 8.1	700 ± 59

Note: ISL = interspinous ligament; Av ± SD = average ± standard deviation.

IV. DISCUSSION

The current study produced a repeatable dynamic experimental testing protocol for investigating the effect of a pre-impact head-forward posture on neck injury risk during inverted drop HFI. In three successful experiments, a nominal head eccentricity of 30 mm with a horizontal FP caused a sequence of head-neck motions and lower-neck ligament failure that culminated in bilateral C7/T1 CFD. Acknowledging the limited sample size, these findings align with the predictions of a recent complementary dynamic FE analysis of HFI. The study showed that a pre-impact head eccentricity exceeding 20 mm, combined with a horizontal FP, generated neck kinematics and

kinetics likely to induce CFD [5]. These data also support the hypothesis of Maiman *et al.* that 'major hyperflexion' injury to the lower neck during HFI is associated with C0-T1 eccentricity of 31 mm, while larger eccentricities (>70 mm) reduce risk of severe neck injury; however, a horizontal FP was not maintained in those experiments [8]. Future studies could utilise this experimental framework to investigate the influence of HFI parameters on CFD risk, such as increased eccentricity, head rotation, or an inclined impact surface, and apply the findings to develop innovative neck injury prevention strategies, which could subsequently be evaluated using the HFI model.

Understanding the mechanics underlying CFD and developing improved approaches to mitigation and treatment is of great contemporary interest [9]. The spinal research communities largely accept that neck dislocation is caused by torso compression during HFI, as evidenced by its association with motor-vehicle rollovers and falls [1][10], yet CFDs are often still classified as a 'hyperflexion' injury caused by head-inertia during whiplash or a downward impact on the top of the head. Despite strong experimental evidence that head flexion alone cannot cause CFD [9], no studies have demonstrated via repeatable experimental frameworks or computational models that HFIs produce lower neck dislocations. Highly controlled, low-rate experimental studies have indicated that anterior head-eccentricity is required for CFD to occur from compression loading [2-3], but this had not been confirmed under dynamic loading conditions.

While CFD has sporadically occurred during previous inverted drop HFI experiments of head-necks, the factors that influenced its occurrence for those particular specimens are unclear [4][11]. Nightingale *et al.* explored the effect of varying impact angle and surface padding on cervical spine mechanics and injuries during HFI [4]. C6/C7 CFD was produced in two out of 22 specimens, both under different experimental conditions: #N18 impacted a rigid surface angled at 15° to horizontal (producing head extension); #N03 impacted a horizontal, padded surface that produced head flexion. Pre-impact head-neck postures were described as 'anatomically neutral', but the exact posture for each specimen is unknown due to the absence of raw kinematic data. In a 2012 study, Ivancic hypothesised that pre-impact head protrusion would produce neck dislocation during horizontal HFI that simulated sports head contact, but CFD only occurred in one of 10 experiments [11]. The precise pre-impact conditions for the specimen that dislocated were not published, but average FP angle and head eccentricity amongst all experiments were 9.6 ± 5.5° and 52 ± 11 mm, respectively.

The low incidence of CFD reported in Ivancic's study is unexpected, as the findings of the present study and complementary computer simulations [5] suggest that the pre-HFI posture would be associated with a high risk of CFD. This discrepancy indicates that differences in Ivancic's experimental setup compared to the current model likely altered head-neck mechanics and influenced CFD risk. Ivancic's study utilised Hybrid III (HIII) heads and a padded impact surface, whereas the current study retained the PMHS heads and impacted a rigid surface. The increased friction of the padded surface and HIII scalp material ($\mu = 0.8$ [12] vs 0.52 for the current experiments [5]) appears to have inhibited the head flexion rotation and anterior translation observed post-ISL failure in the current study (Fig. 3C and E). This head motion generated C7/T1 shear forces (700 ± 59 N) sufficient to cause failure of the anterior longitudinal ligament and cause CFD [13]. Taken together, these results demonstrate the complex interplay of dynamic head-neck motions and subsequent sequence of tissue failure that occurs during CFD from HFI and may suggest that, contrary to prior hypotheses [4], padded impact surfaces *reduce* lower neck injury risk.

Common amongst all studies that have produced CFD during HFI experiments is the complete rupture of all intervertebral soft tissues at the level of dislocation, but a lack of concomitant facet fractures that are observed clinically [14]. It has been suggested that this is an artefact of the lack of passive and active neck musculature in these experimental models, which may increase intervertebral compression and shear forces [15], causing higher inter-facet joint loading and subsequent fracture during CFD [13]. Future studies could investigate this by adding muscle-replicating tension cables to osseoligamentous head-necks in the current model, or by performing the HFI experiments with intact neck musculature.

V. CONCLUSION

To the authors' knowledge, the current study reports the first repeatable experimental model of CFD from HFI and demonstrates that a pre-impact HFP is a risk factor for dislocation injury. High-resolution, dynamic head-neck kinematics and kinetics that caused CFD were collected to inform and validate advanced FE human body models of neck injury, and will assist with developing novel approaches to neck injury prevention.

VI. ACKNOWLEDGEMENTS

The authors would like to thank: L. Sweet, C. Jones, and P. Foroutan for their contributions; The Adelaide Medical School Body Donor Program, anatomical donors and their families; Lifetime Support Authority for project funding (R2230).

VII. REFERENCES

[1] Foroutan, P., Quarrington, R. D., Jones, C. F. (2024) Mechanisms and risk factors associated with spinal cord injury, facet fracture, and level of dislocation, in occupants with cervical spine dislocations sustained in motor vehicle crashes. *Traffic Injury Prevention*, **25**(8): pp. 1129–1136.

[2] Nightingale, R. W., Doherty, B. J., Myers, B. S., McElhaney, J. H., Richardson, W. J. (1991) The influence of end condition on human cervical spine injury mechanisms. SAE Technical Paper 912915.

[3] Bauze, R. J. and Ardran, G. M. (1978) Experimental production of forward dislocation in the human cervical spine. *The Journal of Bone and Joint Surgery* (Br), **60-B**(2): pp. 239–245.

[4] Nightingale, R. W., McElhaney, J. H., Richardson, W. J., Myers, B. S. (1996) Dynamic responses of the head and cervical spine to axial impact loading. *Journal of Biomechanics*, **29**(3): pp. 307–318.

[5] Mongiardini, M., Jones, C., Quarrington, R. D. (2024) The effect of head-forward posture on risk of lower neck dislocation during head-first impacts. *Proceedings of the IRCOBI Conference*, 2024, Stockholm, Sweden.

[6] Eppinger, R., Kuppa, S., Saul, R., Sun, E. (2000) Supplement: development of improved injury criteria for the assessment of advanced automotive restraint systems: II.

[7] Robertson, G., Caldwell, G., Hamill, J., Kamen, G., Whittlesey, S. (2013) Research Methods in Biomechanics, 2E. *Human Kinetics*.

[8] Maiman, D. J., Yoganandan, N., Pintar, F. A. (2002) Preinjury cervical alignment affecting spinal trauma. *Journal of Neurosurgery*, **97**(1 Suppl): pp. 57–62.

[9] Nightingale, R. W., Bass, C. R., Myers, B. S. (2019) On the relative importance of bending and compression in cervical spine bilateral facet dislocation. *Clinical Biomechanics,* **64**: pp. 90–97.

[10] Quarrington, R. D., Jones, C. F., *et al*. (2018) Traumatic subaxial cervical facet subluxation and dislocation: epidemiology, radiographic analyses, and risk factors for spinal cord injury. *The Spine Journal*, **18**(3): pp. 387–398.

[11] Ivancic, P. C. (2012) Head-first impact with head protrusion causes noncontiguous injuries of the cadaveric cervical spine. *Clinical Journal of Sport Medicine*, **22**(5): pp. 390–396.

[12] Stark, N. E. P., Begonia, M., Viano, L., Rowson, S. (2024) The Influence of Headform Friction and Inertial Properties on Oblique Impact Helmet Testing. *Annals of Biomedical Engineering*, **52**(10): pp. 2803–2811.

[13] Quarrington, R. D., Costi, J. J., Freeman, B. J. C., and Jones, C. F. (2021) Investigating the Effect of Axial Compression and Distraction on Cervical Facet Mechanics During Supraphysiologic Anterior Shear. *Journal of Biomechanical Engineering*, **143**(6).

[14] Foster, B. J., Kerrigan, J. R., *et al*. (2012) Analysis of cervical spine injuries and mechanisms for CIREN rollover crashes. *Proceedings of the IRCOBI Conference*, 2012, Dublin, Ireland.

[15] Nightingale, R. W., Sganga, J., Cutcliffe, H., Bass, C. R. (2016) Impact responses of the cervical spine: A computational study of the effects of muscle activity, torso constraint, and pre-flexion. *Journal of Biomechanics*, **49**(4): pp. 558–564.